Biochimica et Biophysica Acta 859 (1986) 209–218
Elsevier

BBA 73209

The static and dynamic behaviour of fluorescent probe molecules in lipid bilayers

F. Mulders, H. van Langen, G. van Ginkel and Y.K. Levine *

Department of Molecular Biophysics, Physics Laboratory and Debye Research Centre, P.O. Box 80.000, 3508 TA Utrecht (The Netherlands)

(Received February 11th, 1986)

Key words: Fluorescence depolarization; Fluorescent probe; Lipid multibilayer; Molecular order; Membrane dynamics

Angle-resolved fluorescence depolarization experiments were carried out on 1,6-diphenyl-1,3,5-hexatriene (DPH) and 1-[4-(trimethylammonium)phenyl]-6-phenyl-1,3,5-hexatriene (TMA-DPH) molecules embedded in multibilayers of dimyristoylphosphatidylcholine (DMPC) and palmitoyloleoylphosphatidylcholine (POPC) above their respective phase transitions. The finding that the order parameter $\langle P_2 \rangle$ of the absorption moment is significantly higher than that for the emission moment for each probe is shown to arise from a tilt of the emission moment relative to the molecular symmetry axis. It is further shown that while the order parameter $\langle P_2 \rangle$ is the same for both probes in DMPC bilayers, it is higher for TMA-DPH than for DPH molecules in POPC bilayers. Considerations of the order parameters $\langle P_4 \rangle$, however, show that this difference can be ascribed solely to the higher fraction of DPH molecules lying with their axes parallel to the bilayer surface. Furthermore it is found that TMA-DPH molecules undergo slower reorientational motions than DPH molecules in the same bilayer system. Nevertheless the motion of both probe molecules is faster in DMPC than in POPC bilayers. The results indicate that TMA-DPH is a more useful probe than DPH in the systems investigated.

Introduction

Fluorescent probes are widely used in studies of the molecular order and dynamics of natural and model membranes [1–6]. In particular the probes 1,6-diphenyl-1,3,5-hexatriene (DPH) and its more polar analogue 1-[4-(trimethylammonium)phenyl]-6-phenyl-1,3,5-hexatriene (TMA-DPH) are often chosen because of their favourable photophysical properties [7–13]. The dynamic behaviour of these molecules in many lipid systems can be adequately described on taking the molecules to possess cylindrical symmetry about their long axes [13,16–18]. The orientational order of the molecules is then characterized by the order parameter $\langle P_2 \rangle = 1/2\langle 3\cos^2\beta - 1 \rangle$ and $\langle P_4 \rangle = 1/8\langle 35\cos^4\beta - 30\cos^2\beta + 3 \rangle$. As the absorption transition moments of the molecules lie parallel to the molecular symmetry axes, fluorescence depolarization experiments sense only the motion of the axes relative to the normal to the plane of the membranes. Although the order parameter $\langle P_2 \rangle$ can be determined directly from the experimental data, the parameter $\langle P_4 \rangle$ and the diffusion constants or rotational correlation times describing the reorientational motion can only be obtained on fitting the experimental observations to a motional model [13,15–18]. The relative orientation of the absorption and emission transition moments in the molecular frame must, however, be known if this information is to be extracted. The relative orientation is expressed in the fundamental anisotropy r_0 [13,18], but it is common to take two moments to be collinear so that $r_0 = 0.4$.

* To whom correspondence should be addressed.

Fluorescence depolarization experiments, in the time or frequency domains, are conveniently carried out on vesicle systems which possess isotropic macroscopic symmetry. However, studies of macroscopically oriented lipid systems can yield more detailed information [13,16–21]. We have previously shown [14–17,19,20] that angle-resolved fluorescence depolarization (AFD) experiments on oriented multibilayers provide an alternative to time-resolved experiments on vesicle systems even under continuous (steady-state) illumination conditions. In these experiments probe molecules lying at different orientations relative to the bilayer normal can be selectively excited by varying the angle of incidence of the excitation beam. At the same time the polarized emission from a selected population of excited molecules can be observed by changing the angle between the directions of incidence and observation. This method affords the determination of the order parameter $\langle P_2 \rangle$ for the absorption moment of the fluorescent probes as well as $\langle P_2 \rangle$ for the emission moment. The two parameters can also be obtained from a combination of linear dichroism and time-resolved fluorescence depolarization experiments utilizing a 90°-scattering geometry [21].

Experiments on DPH molecules embedded in different oriented lipid systems [16,17,19–21] have revealed that $\langle P_2 \rangle$ for the absorption moment differs appreciably from that of the emission moment. If the two moments are parallel in the molecular frame, $r_0 = 0.4$, this indicates that the orientational behaviour of the molecules in the excited state is significantly different from that of the molecules in their ground electronic state [21]. On the other hand, this observation may merely mean that the two moments are not mutually parallel in the molecular frame so that $r_0 < 0.4$ [16,17,19,20].

In order to resolve this problem we have undertaken a study of DPH and TMA-DPH molecules embedded in multibilayers of dimyristoylphosphatidylcholine (DMPC) and palmitoyloleoylphosphatidylcholine (POPC) above their respective phase transitions. Detailed information of the order and dynamics of the probes is obtained on combining steady-state AFD and fluorescence decay measurements on the same sample. It is found that the long life-time decay components of both DPH and TMA-DPH molecules dominate the experimental steady-state signals, so that the method is insensitive to the presence of any fast-decaying photoproducts [11] of the probe molecules.

It is found that a consistent description of the experimental results is obtained either on assuming that the orientational behaviour of the molecules in the excited state differs from that in the ground state [21] or on taking the two transition moments not to be parallel [16,17,29,20]. Both approaches yield the same order parameters $\langle P_2 \rangle$ and $\langle P_4 \rangle$ for the molecules in their ground state, though they lead to somewhat different values for the motional rates.

The results show that while the order parameter $\langle P_2 \rangle$ is the same for both probes in DMPC bilayers, it is higher for TMA-DPH than for DPH molecules in POPC bilayers. However, on taking the order parameter $\langle P_4 \rangle$ into account we show that the differences in the ordering of the probes can be ascribed solely to the different fractions of the probe molecules lying with their axes parallel to the bilayer surface. Furthermore it is found that TMA-DPH molecules undergo slower reorientational motions than DPH molecules in the same lipid bilayer systems. The results strongly indicate that TMA-DPH molecules are more useful probes than DPH in the systems investigated.

Theory

Angle-resolved fluorescence depolarization (AFD) experiments

The theory of the experiment has been discussed in detail elsewhere [15,17,19] and will only be summarized briefly. A macroscopically aligned bilayer system is subjected to continuous illumination with light of defined wavelength and polarization direction. The geometrical arrangement is shown in Fig. 1. The excitation light is incident at an angle θ relative to the macroscopic director and is polarized in the zy-plane. The fluorescence emission is observed at an angle φ with its polarization either parallel ($I_{\parallel}$) or perpendicular ($I_{\perp}$) to the zy-plane. In general the polarizations of the exciting light and the fluorescence emission will not be parallel in the zy-plane. The polarization $R_e = I_{\perp}/I_{\parallel}$ is given by Eqn. 1.

$$R_e = \left[1 - R_1 + (R_3 + R_1)\sin^2\theta\right] \times \left[1 + R_1 + (R_2 - R_1)\sin^2\varphi + (R_3 - R_1)\sin^2\theta + R_5 \sin^2\theta \sin^2\varphi + R_4 \sin 2\theta \sin 2\varphi\right]^{-1} \quad (1)$$

The angles θ and φ and the intensities $I_\perp$ and $I_\parallel$ in Eqn. 1 refer to quantities within the sample and not to those measured in the laboratory system. The angles in the sample and the laboratory can be related simply if the refractive index of the same is known. However, the effects of the sample/air interface on the transmission of light intensity are more complex and depend furthermore on the direction of polarization. The various artefacts have been discussed in detail by Lax and Nelson [22]. It can be easily shown that the effects of multiple reflections of the exciting and emitted light within the sample compensate the transmission losses of the fluorescent light at the interface. Furthermore, consideration of the φ-dependence of the intensities $I_\perp$ and $I_\parallel$ obtained with a normal incidence of the exciting light ($\theta = 0°$), indicate that only solid-angle expansion [22] distorts the experimental results. This effect cancels out on calculating the polarization ratio. Consequently no correction need by applied to the values of R_e determined experimentally.

The polarization ratio R_e is measured for various combinations of θ and φ and affords the determination of five independent quantities S_μ, S_ν, g_0, g_1 and g_2 from steady-state experiments. Here S_μ and S_ν are, respectively, the second rank order parameters ($\equiv \langle P_2 \rangle$) for the absorption and emission transition moments. For DPH and TMA-DPH molecules the quantities g_k, $k = 0, 1, 2$ are defined by

$$g_k = 2.5 r_0 \int_0^\infty G_k(t)\, dt$$

$$G_k(t) = \langle D^2_{k0}(\Omega_\mu)\, D^{2*}_{k0}(\Omega_\nu) \rangle$$

$$\int_0^\infty F(t)\, dt = \int_0^\infty (\alpha_1/\tau_1) \exp(-t/\tau_1) + (\alpha_2/\tau_2) \exp(-t/\tau_2)\, dt = 1 \quad (2)$$

where D^2_{k1} are Wigner rotation matrix elements [23] and Ω_μ and Ω_ν denote, respectively, the orientation of the absorption moment at time $t = 0$ and that of the emission moment at time t, relative to the director frame (Fig. 1). $F(t)$ denotes the normalized intrinsic fluorescence decay function and r_0 is the fundamental anisotropy of the molecules.

The time behaviour of the correlation functions $G_k(t)$ is obtained from models for the reorientational motion of the molecules. It is important to realize that the values of $G_k(t)$ for $t = 0$ and $t \to \infty$ are model independent as a consequence of the assumption that the motion can be described as a stochastic process. These limits can be expressed solely in terms of the order parameters $\langle P_2 \rangle$ and $\langle P_4 \rangle$ [13,24]. The correlation functions $G_1(t)$ and $G_2(t)$ decay to zero at long time, whereas the function $G_0(t)$ decays to a constant value given by $\langle P_2 \rangle^2$.

$F(t)$ can be determined experimentally on observing the fluorescence emission in a direction normal to the sample surface ($\varphi = 0°$) and under an angle of incidence in the sample $\theta = \sin^{-1}(1/\sqrt{3})$. If the polarizer on the emission side is set with its optical axis at 45° to the vertical, then the combined signal $I_\perp + I_\parallel$ is proportional to $F(t)$ [15].

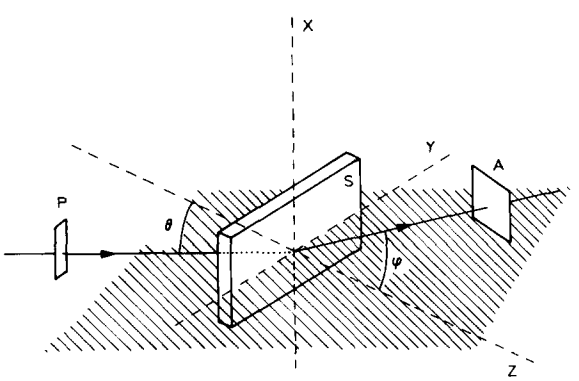

Fig. 1. Experimental AFD geometry for a lamellar bilayer sample S lying in the *xy*-plane. θ and φ are the angles in air between the normal to the planes of the bilayers *z* and, respectively, the directions of exciation and observation of the fluorescence. The states of polarization, either parallel or perpendicular to the *zy*-plane are determined by the polarizer P and the analyzer A. The angles θ and φ (taken to be positive as drawn) change sign on rotation of the light beams through the *z*-axis.

Orientation of molecules in membrane systems

We shall here consider the case of a uniaxial bilayer system containing cylindrically symmetric probe molecules. The orientation of the molecules

in the system is specified by the angle β between the molecular symmetry axes and the bilayer normal [25]. The orientational distribution of an average molecule in the system is then characterized by a probability distribution $f(\beta)$. This distribution can be expressed as a series expansion of Legendre polynomials $P_L(\cos\beta)$, each of which is weighted by an order parameter $\langle P_L \rangle$ which is the ensemble average of the corresponding term

$$f(\beta) = 1/2 \sum_{L=0}^{\infty} (2L+1)\langle P_L \rangle P_L(\cos\beta); \quad L \text{ even} \tag{3}$$

$$f(\beta) \geq 0; \quad \int_0^{\pi} f(\beta) \sin\beta \, d\beta = 1$$

$$\langle P_L \rangle = \int_0^{\pi} f(\beta) P_L(\cos\beta) \sin\beta \, d\beta$$

The orientational distribution function $f(\beta)$ is fully characterized if all the order parameters $\langle P_L \rangle$ are known. In practice, however, only $\langle P_2 \rangle$ and $\langle P_4 \rangle$ are accessible experimentally.

The main difficulty now is obtaining an objective and realistic estimate of the form of $f(\beta)$ from limited knowledge of its moments. This may be accomplished by an information-theoretic approach [15,26,27]. The essential point is, that given the order parameters $\langle P_2 \rangle$ and $\langle P_4 \rangle$, the most probable values of $\langle P_L \rangle$, $L \geq 6$, are calculated under the assumption that the informational entropy of $f(\beta)$ is a maximum. This corresponds to the construction of the broadest possible distribution function consistent with the known values of $\langle P_2 \rangle$ and $\langle P_4 \rangle$. It can then be shown that the resulting distribution function has the form

$$f(\beta) = A \exp[\lambda_2 P_2(\cos\beta) + \lambda_4 P_4(\cos\beta)] \tag{4}$$

where A is a normalization constant and λ_2 and λ_4 are determined from the known values of $\langle P_2 \rangle$ and $\langle P_4 \rangle$. If only the order parameter $\langle P_2 \rangle$ is known, the distribution function takes the form of Eqn. 4 but with $\lambda_4 = 0$. We note here that Eqn. 4 has the form of a Boltzmann distribution with an angle-dependent orienting potential.

It can be seen from Eqn. 4 that if only $\langle P_2 \rangle$ is known, the reconstructed distribution function either has a maximum at $\beta = 0$ and decreases monotonically to a minimum at $\beta = \pi/2$ or vice versa. Knowledge of $\langle P_4 \rangle$ is required for establishing the existence of a collective molecular tilt which is manifested by a maximum of the distribution function at an angle intermediate between 0 and $\pi/2$. On the other hand the observation of a minimum at such an angle may be taken as an indication for a superposition of two or more independent populations of molecules. The available information, however, is too limited to allow their resolution.

Models for reorientational motion

We shall here consider two models for the dynamical behaviour of the probe molecules: the strong-collision (SC) [13,15] and the rotational diffusion (RD) model [13,18].

(A) Strong-collision model

The probe molecules are assumed to undergo uncorrelated, random rotational jumps with a residence time τ_c in any orientation. The correlation functions $G_k(t)$ decay exponentially and independently of k as

$$G_k(t) = [G_k(t) - G_k(\infty)]\exp(-t/\tau_c) + G_k(\infty) \tag{5}$$

$k = 0, 1, 2$

(B) Rotational diffusion model

Here the molecules are assumed to undergo small step rotational diffusion subject to an anisotropic orienting potential $U(\beta)$. In view of the discussion above on the reconstruction of the equilibrium orientation distribution function, we shall choose $U(\beta)$ to take the form

$$U(\beta) = -kT\{\lambda_2 P_2(\cos\beta) + \lambda_4 P_4(\cos\beta)\} \tag{6}$$

We note that our choice of the orienting potential spans all the physically permissible pairs of $(\langle P_2 \rangle, \langle P_4 \rangle)$ values. It is important to realize that this model does not presuppose sticky boundary conditions for which an interpretation in terms of viscosity is valid.

The correlation functions are now given as a sum of exponential decays

$$G_k(t) = \sum_M b_M^k \exp(-D_\perp \alpha_M^k t) \tag{7}$$

where the amplitudes b_M^k and the exponential

factors α_M^k are determined by λ_2 and λ_4. $D_\perp$ is the diffusion coefficient of the symmetry axis of the molecule.

In many practical situations, the correlation functions $G_k(t)$ are found to have a monoexponential decay of the form of Eqn. 5, but with a separate correlation time for each k [13,18].

Materials and Methods

Dimyristoylphosphatidylcholine (DMPC) and palmitoyloleoylphosphatidylcholine(POPC) were purchased from Sigma Chemical Co. and used without further purification.

The probe 1,6-diphenyl-1,3,5-hexatriene (DPH) was obtained from Fluka (Buchs, Switzerland). The purity was controlled by reversed-phase HPTLC. TMA-DPH was purchased from Molecular Probes, Inc. (Plano, TX, U.S.A.).

The probes were dissolved in absolute ethanol and stored in the dark at 4°C.

Sample preparation

Macroscopically ordered membrane systems were prepared from DMPC or POPC + ≈ 25% water as described in [17] and [19]. DPH and TMA-DPH embedded in the membrane are used as fluorescent probes. The probe to lipid ratio was 1 : 250 on a molecular basis.

The membrane systems were kept in the dark as much as possible and were only exposed to daylight during the alignment procedure and on being mounted in the sample holder.

AFD measurements

Angle-resolved fluorescence depolarization (AFD) experiments were carried out at the temperatures indicated on a home-built fluorimeter described by Van Ginkel [29] and modified for AFD measurements. Basically it consists of a Xenon arc (Osram XBO 1600 W), a 0.25 m Jarrel-Ash grating monochromator and a Peltier-cooled RCA 31034 PM tube, operating at approximately −25°C and a cathode voltage of −1250 V. The angles θ and φ (see Fig. 1) were set to within 1° by two goniometers on which the sample holder and the PM tube assembly were independently mounted.

The probes were excited at 380 nm (monochromator + Balzers interference filter with 8 nm halfwidth). The PM-tube was equipped with a Schott GG-395 cut-off filter and a Balzers 432 nm interference filter (12 nm halfwidth) to detect fluorescence emission of the probes. The fluorescence emission signal from the PM-tube was amplified by a PAR 186A-lock-in-amplifier and then fed directly into an Apple II microcomputer for storage and handling of the data.

The sample was excited at an angle of incidence θ with light polarized in the zy-plane and the fluorescence emission was detected with a polarization parallel ($I_\parallel$) and perpendicular ($I_\perp$) to the zy-plane at angle φ (see Fig. 1). The polarization ratio $R_e = I_\perp / I_\parallel$ was measured for 56 combinations of θ and φ.

Fluorescence decay measurements were carried out with a similar set-up using an Edinburgh Instruments 399 flash lamp operating with N_2 gas at atmospheric pressure as a light source and a single photon counting detection system (Ortec). The fluorescence decay law was extracted from the measurements using POPOP as a reference compound and following the procedure of Zucker et al. [31] for data analysis.

TABLE I

PARAMETERS

System	R_1	R_2	R_3	R_4	R_5	$\alpha_1 = 1 - \alpha_2$	τ_1 (ns)	τ_2 (ns)
DMPC/DPH	0.1166	1.699	3.566	0.3416	11.17	–	–	8.21
POPC/DPH	0.1770	0.7778	2.311	0.2482	5.949	0.05	1.62	7.6
DMPC/TMA-DPH	0.1681	2.305	2.892	1.020	19.08	0.03	0.54	5.8
POPC/TMA-DPH	0.2840	1.538	2.859	1.282	18.62	0.19	1.0	4.8

Results and Discussion

AFD experiments were carried out for DPH and TMA-DPH molecules embedded in multibilayers of DMPC and POPC. The same values of the polarization ratios R_e, within the experimental error of 2%, were obtained on rotating the samples by an arbitrary angle about the normal to their surfaces. The fluorescence intensity, measured at the same scattering geometry, remained constant during the experiments.

Orientation of the transition moments

The parameters R_1–R_5 were determined from the experimental values of R_e as described in Refs. 17 and 19, and are shown in Table I. The quantities S_μ, S_ν, g_0, g_1, g_2 were obtained on taking linear combinations of R_1–R_5 [15].

The analysis shows that in all the systems studied $S_\mu > S_\nu$ for both DPH and TMA-DPH in accordance with our previous studies [16,17,19,20] and the recent finding of Johansson [21] in other oriented lipid systems.

In order to examine the origin of this difference we evaluated the correlation functions (Eqn. 2) in terms of the analytical expressions of the strong-collision (SC) model (Eqn. 5). We thus find

$$g_k = 2.5 r_0 \{ w G_k(0) + (1-w) G_k(\infty) \}$$

$$k = 0, 1, 2$$

$$w = \int_0^\infty F(t) \exp(-t/\tau_c)\, dt \qquad (8)$$

The function $G_k(0)$ can be expressed solely in terms of the order parameters $\langle P_2 \rangle$ and $\langle P_4 \rangle$ [13,18] and $0 \leqslant w \leqslant 1$.

If we now assume that the orientational distribution function of the molecules in the excited state $f_{ex}(\Omega)$ differs from that in the ground state $f_g(\Omega)$ as proposed by Johansson we find [13,15,18,21]

$$G_k(\infty) = \langle P_2 \rangle_g \langle P_2 \rangle_{ex} \delta_{k0}$$

$$S_\nu = (1-w) \langle P_2 \rangle_{ex} + w \langle P_2 \rangle_g$$

$$S_\mu = \langle P_2 \rangle_g$$

where $\langle \ldots \rangle_g$ and $\langle \ldots \rangle_{ex}$ denote averaging over, respectively, the ground and excited state distribution functions. On taking $r_0 = 0.4$, transition moments parallel, we can now solve for $\langle P_2 \rangle_g$, $\langle P_2 \rangle_{ex}$, $\langle P_4 \rangle_g$ and τ_c and the results are given in Table II for all the systems studied. We note that the solution is self-consistent, so that the same correlation time describes the decay of both the correlation functions $G_k(t)$ as of the order parameter S_ν.

However, if we assume that the emission moment, ν, is tilted by an angle β_ν with respect to the absorption moment, μ, and hence to the molecular symmetry axis and that furthermore $f_{ex}(\Omega) = f_g(\Omega)$ we find

$$G_k(\infty) = \langle P_2 \rangle^2 \delta_{k0}$$

$$S_\nu = \langle P_2 \rangle P_2(\cos \beta_\nu)$$

$$S_\mu = \langle P_2 \rangle \qquad (10)$$

where $P_2(\cos \beta_\mu) = 2.5\ r_0$. The values for $\langle P_2 \rangle$, $\langle P_4 \rangle$, r_0 and τ_c now obtained are given in Table II.

Inspection of Table II shows that both approaches yield the same results for the order parameters $\langle P_2 \rangle_g$ and $\langle P_4 \rangle_g$, though they lead to somewhat different values for the correlation times

TABLE II

ORDER AND DYNAMICS OBTAINED FROM THE STRONG-COLLISION (SC) MODEL

Lipid + probe	Transition moments parallel, excited state and ground state not equivalent				Transition moments tilted, excited state and ground state equivalent			
	$\langle P_2 \rangle_g$	$\langle P_2 \rangle_{ex}$	$\langle P_4 \rangle_g$	τ_c (ns)	$\langle P_2 \rangle_g$	$\langle P_4 \rangle_g$	τ_c (ns)	r_0
DMPC + DPH	0.61	0.42	0.36	1.8	0.61	0.36	2.5	0.30
POPC + DPH	0.52	0.26	0.42	2.4	0.53	0.42	4.3	0.26
DMPC + TMA-DPH	0.65	0.60	0.26	3.1	0.65	0.27	3.2	0.37
POPC + TMA-DPH	0.66	0.46	0.35	5.6	0.67	0.36	7.2	0.34

τ_c. Nevertheless the results clearly show that the same conclusions about the dynamic behaviour of the probes can be drawn from both approaches. It is interesting to note that the model of Johansson [21] indicates that the differences between the ground and excited state distribution functions is more pronounced in POPC bilayers than in DMPC bilayers for both PDH and TMA-DPH molecules. This difference is manifested as a decrease in the r_0 values in the approach proposed by us previously [16,17,19,20].

In view of our finding above that both approaches yield the same conclusions about the dynamic behaviour of the probes, we shall analyse the results further on taking the transition moments of the molecules to be non-collinear.

Data analysis

Numerical values for the various model parameters were obtained from a direct fit of the model of motion to the experimental data with a nonlinear least-squares method using the measured fluorescence decay behaviour shown in Table I. The strong-collision (SC) model requires the use of $\langle P_2 \rangle$, $\langle P_4 \rangle$, $P_2(\cos \beta_\nu)$ and τ_c as free parameters, while λ_2, λ_4, $D_\perp$ and $P_2(\cos \beta_\nu)$ were used as free parameters for fitting the rotational diffusion (RD) model. The derived values of the parameters are summarized in Table III. Note that the correlation times τ_k, $k = 0, 1, 2$ given for the RD model are defined as the area under the time-dependent part of the correlation function $G_k(t)$.

Importantly, we have found that the values shown change by less than 5% if the fluorescence decay function was taken to be monoexponential with a lifetime equal to τ_2 for the long decay component. It is thus permissible to analyze the experimental data without prior knowledge of the fluorescence decay and on taking $F(t)$ to be a monoexponential function. In this case the model parameters become τ_c/τ_F and $D_\perp \tau_F$ for the SC and RD models, respectively.

The analyses show that both models can be used to describe the dynamic behaviour of the probe molecules in the lipid system, although it is difficult to discriminate between them. Nevertheless the results in Table III clearly show that the same conclusions about the dynamic behaviour of the probe molecules can be drawn from the models.

Orientational order

In POPC bilayers at 21°C the order parameter $\langle P_2 \rangle$ for DPH is significantly lower than that for TMA-DPH, but this difference is considerably smaller for DMPC bilayers at 35°C. Although the value of $\langle P_2 \rangle$ for DPH in DMPC bilayers is higher than that in POPC bilayers, similar values are observed for TMA-DPH in these systems.

The differences in the $\langle P_2 \rangle$ values for the two probe molecules in the same system have been ascribed to differences in locations in the bilayer structure [30]. Indeed we expect the TMA-DPH molecules to be anchored in the headgroup region of the bilayer [12,30], while the more lipophilic DPH molecules may be found in other locations and move freely up and down the bilayer along the lipid chains. It is important to note in this context that space filling models show that the length of the probe molecules is of the same order as the length of the fatty acid chains of the lipids, Fig. 2. In order to gain insight into the orienta-

TABLE III

COMPARISON OF ORDER AND DYNAMICS OBTAINED FROM STRONG-COLLISION (SC) AND ROTATIONAL DIFFUSION (RD) MODELS

Lipid + probe	SC model				RD model							Temp. (°C)	$\frac{f(90)}{f(0)}$ (%)
	β_ν	$\langle P_2 \rangle$	$\langle P_4 \rangle$	τ_c (ns)	β_ν	$\langle P_2 \rangle$	$\langle P_4 \rangle$	$D_\perp$ (ns^{-1})	τ_0 (ns)	τ_1 (ns)	τ_2 (ns)		
DMPC + DPH	24	0.61	0.36	2.5	24	0.60	0.31	0.045	4.4	2.3	2.5	35	2
POPC + DPH	29	0.53	0.42	4.3	30	0.52	0.30	0.034	8.6	3.1	4.1	21	4
DMPC + TMA-DPH	12	0.65	0.27	3.2	12	0.64	0.29	0.035	3.9	3.5	2.6	35	0.75
POPC + TMA-DPH	18	0.67	0.36	7.2	18	0.66	0.35	0.014	7.2	7.2	6.9	21	0.80

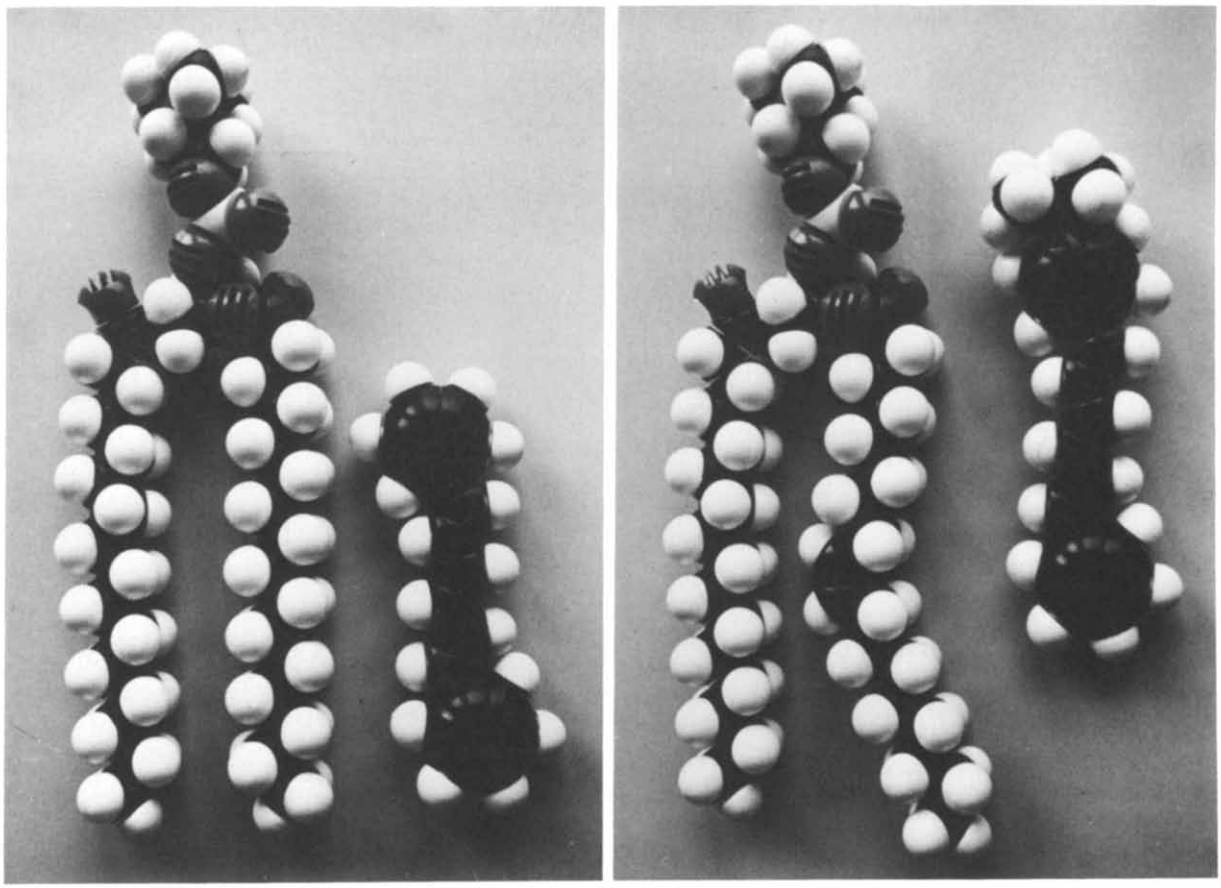

Fig. 2. Space filling models of (from left to right): DMPC, DPH, TMA-DPH and POPC molecules.

tional distribution of the molecules in the bilayer system we have reconstructed the orientational distribution function $f(\beta)$ (Eqn. 4) from the values of $\langle P_2 \rangle$ and $\langle P_4 \rangle$ (Table II). Figs. 3 and 4 show the functions for DMPC and POPC bilayers, respectively. It can be seen from Fig. 3 that both probe molecules have a similar distribution function in DMPC bilayers. The distribution decreases monotonically from a maximum at $\beta = 0°$ (molecules perpendicular) to the bilayer surface to $\beta = 90°$ (molecular axes parallel to the bilayer surface). Interestingly, a greater fraction (2%) of DPH molecules are to be found at $\beta = 90°$, compared to TMA-DPH molecules, 0.75%.

The distribution function for DPH molecules in POPC bilayers, on the other hand, exhibits a distinct minimum at $\beta \approx 60°$, in marked contrast to the distribution of TMA-DPH molecules. In particular 4% of the DPH molecules are found to lie with their axes parallel to the bilayer surface compared to 0.8% TMA-DPH molecules. The form of $f(\beta)$ for DPH molecules is strongly indicative of the presence of at least two distinct populations in the bilayer. It is important to note that the differences in the $\langle P_2 \rangle$ values for DPH and TMA-DPH found in POPC bilayers can be simply and directly ascribed to the higher fraction of DPH molecules than TMA-DPH molecules lying at $\beta = 90°$. These fractions make a large negative contribution to the integral (Eqn. 3) defining the order parameter $\langle P_2 \rangle$.

The question as to the transverse location of the populations of DPH molecules in the bilayer structure, cannot be answered with these experiments. In view of the lipophilic structure of the DPH molecules and recent experiments utilizing

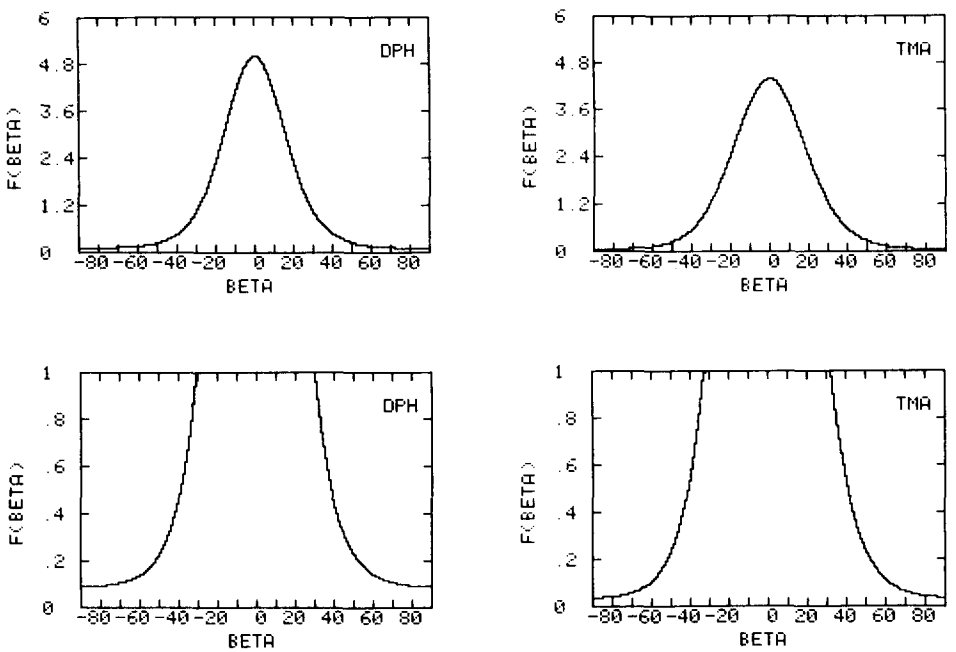

Fig. 3. The orientational distribution functions of DPH (left) and TMA-DPH molecules in DMPC multibilayers at 35°C. The bottom figures show enlarged plots to emphasize the form of the distribution for molecules lying with their axes nearly parallel to the bilayer surface.

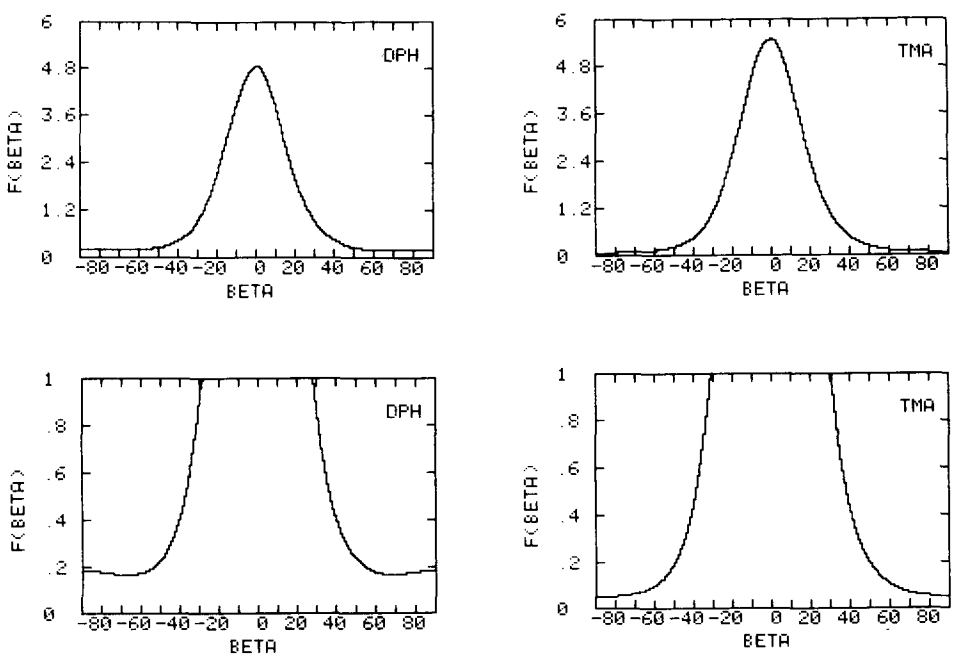

Fig. 4. The orientational distribution functions of DPH (left) and TMA-DPH molecules in POPC multibilayers at 21°C. The bottom figures show enlarged plots to emphasize the form of the distribution for molecules lying with their axes nearly parallel to the bilayer surface.

energy transfer techniques [32] it is likely that DPH molecules are accommodated in the centre of the bilayer structure between the two monolayers. The finding of a variable population of DPH molecules lying with their axes parallel to the bilayer surface is consistent with earlier observations [33,34] of a similar behaviour of β-carotene molecules in lipid bilayer systems. β-Carotene molecules are chemically similar to DPH molecules, but possess a longer conjugated bond structure.

Reorientational dynamics

Both models show that DPH molecules undergo faster reorientational motion than TMA-DPH molecules in the same bilayer system, Table III. Furthermore both probe molecules appear to undergo faster motions in DMPC bilayers at 35°C (T_c + 12) than in POPC bilayers at 21°C (T_c + 26). This slowing down of the dynamics in the presence of unsaturation in the lipid chains has been reported by us previously [19,20]. We note, however, that the comparison of the dynamics of DPH molecules in different bilayer systems may not be valid as a consequence of the presence of a variable fraction of molecules lying with their axes parallel to the bilayer surface. We are therefore forced to conclude that TMA-DPH is a more useful probe for investigations of the dynamic structure of lipid bilayers.

References

1 Yguarabide, J. and Foster, M.C. (1978) in Membrane Spectroscopy (Grell, E., ed.), pp. 199–269, Springer Verlag, New York
2 Shinitzky, M., Dianoux, A.C., Gitler, C. and Weber, G. (1971) Biochemistry 10, 2106–2113
3 Shinitzky, M. and Barenholz, Y. (1978) Biochim. Biophys. Acta 515, 367–394
4 Brand, L. and Gohlke, J.R. (1972) Annu. Rev. Biochem. 41, 843–868
5 Radda, G.K. and Vanderkooi, J. (1972) Biochim. Biophys. Acta 265, 509–549
6 Lakowicz, J.R. (1980) J. Biochem. Biophys. Methods 2, 91–119
7 Shinitzky, M., Barenholz, Y. (1974) J. Biol. Chem. 249, 2652–2657
8 Cehelnik, E.D., Cundall, R.B., Lockwood, J.R. and Palmer, T.F. (1975) J. Phys. Chem. 79, 1369–1376
9 Prendergast, F.G. (1983) Period. Biol. 83, 69–79
10 Prendergast, F.G., Haugland, R.P. and Callahan, P.J. (1981) Biochemistry 20, 7333–7338
11 Barrow, D.A. and Lentz, B.R. (1984) Biophys. J. 48, 221–234
12 Cranney, M., Cundall, R.B., Jones, G.R., Richards, J.T. and Thomas, E.W. (1983) Biochim. Biophys. Acta 735, 418–425
13 Zannoni, C., Arcioni, A. and Cavatorta, P. (1983) Chem. Phys. Lipids 32, 179–250
14 Kooyman, R.P.H., Levine, Y.K. and Van der Meer, B.W. (1981) Chem. Phys. 60, 317–326
15 Van der Meer, B.W., Kooyman, R.P.H. and Levine, Y.K. (1982) Chem. Phys. 66, 39–50
16 Vos, M.H., Kooyman, R.P.H. and Levine, Y.K. (1983) Biochem. Biophys. Res. Commun. 116, 462–468
17 Kooyman, R.P.H., Vos, M.H. and Levine, Y.K. (1983) Chem. Phys. 81, 461–472
18 Szabo, A. (1984) J. Chem. Phys. 81, 150–167
19 Van de Ven, M.J.M. and Levine, Y.K. (1984) Biochim. Biophys. Acta 777, 283–296
20 Van de Ven, M.J.M., Van Ginkel, G. and Levine, Y.K. (1984) Biochem. Biophys. Res. Commun. 123, 352–357
21 Johansson, L.B.-Å. (1985) Chem. Phys. Lett. 118, 516–521
22 Lax, M. and Nelson, D.F. (1973) in Coherence and Quantum Optics (Mandel, L. and Wolf, E., eds.), pp. 415–445, Plenum Press, New York
23 Rose, M.F. (1957) Elementary Theory of Angular Momentum, J. Wiley and Sons, New York
24 Zannoni, C. (1979) Mol. Phys. 83, 1813–1827
25 Zannoni, C. (1981) in The Molecular Physics of Lipid Crystals (Luckhurst, G.R. and Gray, G.W., eds.), Academic Press, New York
26 Berne, B.J. (1971) in Physical Chemistry, an Advanced Treatise (Eyring, H., Henderson, D. and Jost, W., eds.), Vol. 8B, Academic Press, New York
27 Levine, R.D. and Tribus, M. (eds.) (1979) The Maximum Entropy Formalism, M.I.T. Press, Cambridge
28 Nordio, P.L. and Segre, U. (1979) in The Molecular Physics of Liquid Crystals (Luckhurst, G.R. and Gray, G.W., eds.), pp. 411–426 Academic Press, New York
29 Van Ginkel, G. (1977) Acta Bot. Neerl. 26, 303–311
30 Engel, L.W. and Prendergast, F.G. (1981) Biochemistry 20, 7338–7345
31 Zucker, N., Szabo, A.G., Bramall, L., Krajcarski, D.T. and Selinger, B. (1985) Rev. Sci. Instrum. 56, 14–27
32 Davenport, L., Dale, R.E., Bisby, R.H. and Cundall, R.B. (1985) Biochemistry 24, 4097–4108
33 Johansson, L.B.-Å., Lindblom, G., Wieslander, A. and Arvidson, G. (1981) FEBS Lett. 128, 97–99
34 Van de Ven, M., Kattenberg, M., Van Ginkel, G. and Levine, Y.K. (1984) Biophys. J. 45, 1203–1210